



**Title:** Structural and Biophysical Characterization of SARS-CoV-2 Spike Glycoprotein (P2 S) as a Vaccine Antigen

**Study Number:** N/A

**Parent Compound Number(s):** PF-07302048

**Alternative Compound Identifiers:** N/A

**Pfizer Discovery Sciences  
Eastern Point Road  
Groton, CT**

**Title:** Structural and Biophysical Characterization of SARS-CoV-2 Spike Glycoprotein (P2 S) as a Vaccine Antigen

**PRINCIPAL INVESTIGATOR:** (b) (6)

**CONTRIBUTING SCIENTIST(S):**

(b) (6)

**PREPARED BY:**

(b) (6)

**APPROVED BY:**

(b) (6)

**Title:** Structural and Biophysical Characterization of SARS-CoV-2 Spike Glycoprotein (P2 S) as a Vaccine Antigen

**SYNOPSIS**

The binding and structural analysis of SARS-CoV-2 P2 S expressed from DNA that encodes the same amino acid sequence as BNT162b2 RNA indicate that the encoded P2 S antigen authentically presents the ACE2 binding site and other epitopes targeted by SARS-CoV-2 neutralizing antibodies.

090177e195e446ea\Approved\Approved On: 27-Dec-2020 02:23 (GMT)

## TABLE OF CONTENTS

SYNOPSIS.....	3
LIST OF TABLES.....	4
LIST OF FIGURES .....	4
1. OBJECTIVES.....	5
2. INTRODUCTION .....	5
3. MATERIALS AND METHODS.....	6
3.1. Flow Cytometry Analysis of Binding to Cell Surface-Expressed P2 S .....	6
3.2. P2 S Expression and Purification .....	6
3.3. Binding Kinetics of P2 S to Immobilized Human ACE2 and a Neutralizing Monoclonal Antibody by Biolayer Interferometry.....	6
3.4. Cryo-EM of P2 S.....	7
4. RESULTS AND DISCUSSION.....	9
5. CONCLUSION.....	12
6. DEVIATIONS .....	12
7. REFERENCES .....	12

## LIST OF TABLES

Table 1.	CryoEM Data Collection, 3D Reconstruction and Refinement Statistics.....	8
----------	--	---

## LIST OF FIGURES

Figure 1.	Binding to Cell Surface-Expressed Recombinant P2 S.....	9
Figure 2.	Biolayer Interferometry Sensorgrams for Binding of P2 S to ACE2-PD and B38 mAb.....	10
Figure 3.	CryoEM P2 S Structure at 3.29 Å Resolution .....	11

**Title:** Structural and Biophysical Characterization of SARS-CoV-2 Spike Glycoprotein (P2 S) as a Vaccine Antigen

**Study Number:** N/A

**Functional Area:** Medicinal Sciences

**Test Facility:** Pfizer Discovery Sciences, Eastern Point Road,  
Groton, CT

**Study/Testing Initiation Date:** 07April2020

**Study/Testing Completion Date:** 19Aug2020

## 1. OBJECTIVES

The purpose of this study was to express and characterize the vaccine antigen encoded by BNT162b2.

## 2. INTRODUCTION

The coronavirus disease 2019 (COVID-19) vaccine (BioNTech code number BNT162, Pfizer code number PF-07302048) is an investigational vaccine intended to prevent COVID-19, which is caused by severe acute respiratory syndrome coronavirus 2 (SARS-CoV-2). Coronavirus S is a major target of virus neutralizing antibodies and is a key antigen for vaccine development. S is a transmembrane glycoprotein responsible for receptor recognition, attachment to the cell, and viral envelope fusion with a host cell membrane resulting in genome release. While the membrane-proximal S2 is responsible for membrane fusion, the membrane-distal S1, with its receptor-binding domain (RBD), recognizes the host receptor, angiotensin converting enzyme 2 (ACE2) (Zhou et al, 2020). The RBD forms membrane distal “heads” on the S trimer that are connected to the body by a hinge. In the native S, the RBD alternates between an open (up) and closed (down) position. Although potent neutralizing epitopes have been described when the RBD is in the “heads down” closed conformation, the “heads up” receptor accessible conformation exposes a potentially greater breadth of neutralizing antibody targets (Brouwer et al, 2020; Liu et al, 2020; Robbani et al, 2020).

The glycoprotein encoded by the vaccine candidate BNT162b2 includes two amino acid substitutions to proline (P2 S) locking the transmembrane protein in an antigenically optimal prefusion conformation (Pallesen et al, 2017; Wrapp et al, 2020). The P2 S antigen was expressed from DNA and characterized for structure and binding to human ACE2 and SARS-CoV-2 neutralizing antibodies.

### 3. MATERIALS AND METHODS

#### 3.1. Flow Cytometry Analysis of Binding to Cell Surface-Expressed P2 S

A modified pcDNA3.1 Zeo (+) construct encoding the P2 S antigen under control of a CAG promoter was expressed in Expi293F cells as per the supplied Expifectamine 293 Transfection Kit protocol.

Cells were collected 48 hr post transfection, washed with TBS buffer, and used at  $4-5 \times 10^4$  for each condition. Cells were incubated for 1 hr at room temperature (RT) in TBS + 4% BSA + 0.01 mg/mL 7-AAD to detect non-viable cells and with either (i) 1:100 FITC-labeled anti-6xHis plus 10 nM His-tagged human ACE2 peptidase domain (ACE2-PD); (ii) 100 nM Alexa-488 labeled anti-Rabbit IgG Fab plus either 33 nM anti-SARS-CoV-2 Spike RBD ( $\alpha$ RBD, Sino Biological 40592-T62), anti-SARS-Cov-2 Spike S1 ( $\alpha$ S1, Sino Biological 40150-R007), or anti-SARS Spike S2 ( $\alpha$ S2, Novus NB100-56578); or (iii) 100 nM Alexa-488 labeled anti-Human IgG Fab plus either 33 nM CR3022 therapeutic antibody ( $\alpha$ CR3022) (Yuan et al, 2020), B38 neutralizing antibody ( $\alpha$ B38), or H4 neutralizing antibody ( $\alpha$ H4) (Wu et al, 2020). Cells were washed with TBS and then analyzed in a V-bottom 96-well plate using a Guava EasyCyte HT flow cytometry system. For each condition, three replicates were measured with 3000 events collected per replicate.

#### 3.2. P2 S Expression and Purification

To express SARS-CoV-2 P2 S encoded by BNT162b2 for biophysical characterization, a gene encoding the full length SARS-CoV-2 spike (GenBank: MN908947) with two prolines substituted at residues 986 and 987 (K986P and V987P) followed with a C-terminal HRV3C protease site and a TwinStrep tag was cloned into a modified pcDNA3.1(+) vector with the CAG promoter. The TwinStrep-tagged P2 S was expressed in Expi293F cells.

Purification of the recombinant protein was based on a procedure described previously, with minor modifications (Cai et al, 2020). Upon cell lysis, P2 S was solubilised in 1% NP-40 detergent. The TwinStrep-tagged protein was then captured with StrepTactin Sepharose HP resin in 0.5% NP-40. P2 S was further purified by size-exclusion chromatography and eluted as three distinct peaks in 0.02 % NP-40 as previously reported (Cai et al, 2020). A peak that consists of intact P2 S migrating at around 150 kDa, as well as dissociated S1 and S2 subunits (which co-migrate at just above 75 kDa), was used in the structural characterization. Spontaneous dissociation of the S1 and S2 subunits occurs throughout the course of protein purification, starting at the point of detergent-mediated protein extraction, so that P2 S preparations also contain dissociated S1 and S2.

#### 3.3. Binding Kinetics of P2 S to Immobilized Human ACE2 and a Neutralizing Monoclonal Antibody by Biolayer Interferometry

Binding of NP-40 solubilized, purified P2 S to ACE2-PD and human neutralizing monoclonal antibody B38 (Wu et al, 2020) was measured by biolayer interferometry at 25 °C on an Octet RED384 (FortéBio). P2 S binding was measured in 25 mM Tris pH 7.5, 150 mM NaCl, 1 mM EDTA and 0.02% NP-40. Avi-tagged human ACE2-PD was immobilized on streptavidin-coated sensors; B38 antibody was immobilized on protein G-coated sensors. For

a P2 S concentration series, after initial baseline equilibration of 120 seconds, the sensors were dipped in a 10 µg/mL solution of Avi-tagged ACE2-PD or B38 mAb for 300 seconds to achieve capture levels of 1 nM using the threshold function. Then, after another 120 seconds of baseline, binding data were collected for 300 seconds of association and 600 seconds of dissociation.

Biolayer interferometry data were collected with Octet Data Acquisition software version 10.0.0.87 and processed using FortéBio Data Analysis software version 10.0. Data were reference subtracted and fit to a 1:1 binding model with  $R^2$  value greater than 0.95 to determine kinetics and affinity of binding using Octet Data Analysis Software v10.0 (FortéBio).

### 3.4. Cryo-EM of P2 S

For TwinStrep-tagged P2 S, 4 µL purified protein at 0.5 mg/mL were applied to gold Quantifoil R1.2/1.3 300 mesh grids freshly overlaid with graphene oxide. The sample was blotted using a Vitrobot Mark IV for 4 seconds with a force of -2 before being plunged into liquid ethane cooled by liquid nitrogen. 27,701 micrographs were collected from two identically prepared grids. Data were collected from each grid over a defocus range of -1.2 to -3.4 µm with a total electron dose of 50.32 and 50.12 e<sup>-</sup>/Å<sup>2</sup>, respectively, fractionated into 40 frames over a 6-second exposure for 1.26 and 1.25 e<sup>-</sup>/Å<sup>2</sup>/frame. On-the-fly motion correction, CTF estimation, and particle picking and extraction with a box size of 450 pixels were performed in Warp (Tegunov & Cramer, 2019), during which super-resolution data were binned to give a pixel size of 0.87 Å. A total of 1,119,906 particles were extracted. All subsequent processing was performed in RELION 3.1-beta (Zivanov et al, 2018). Particle heterogeneity was filtered out with 2D and 3D classification, yielding a set of 73,393 particles, which refined to 3.6 Å with C3 symmetry. 3D classification of this dataset without particle alignment separated out one class with a single RBD up, representing 15,098 particles. The remaining 58,295 particles, in the three RBD ‘down’ conformation, were refined to give a final model at 3.29 Å. The atomic model from PDB ID 6XR8 (Cai et al, 2020) was rigid-body fitted into the map density, then flexibly fitted to the density using real-space refinement in Phenix (Adams et al, 2010) alternating with manual building in Coot (Emsley et al, 2010). Data collection, 3D reconstruction and model refinement statistics are listed in Table 1.

**Table 1. CryoEM Data Collection, 3D Reconstruction and Refinement Statistics**

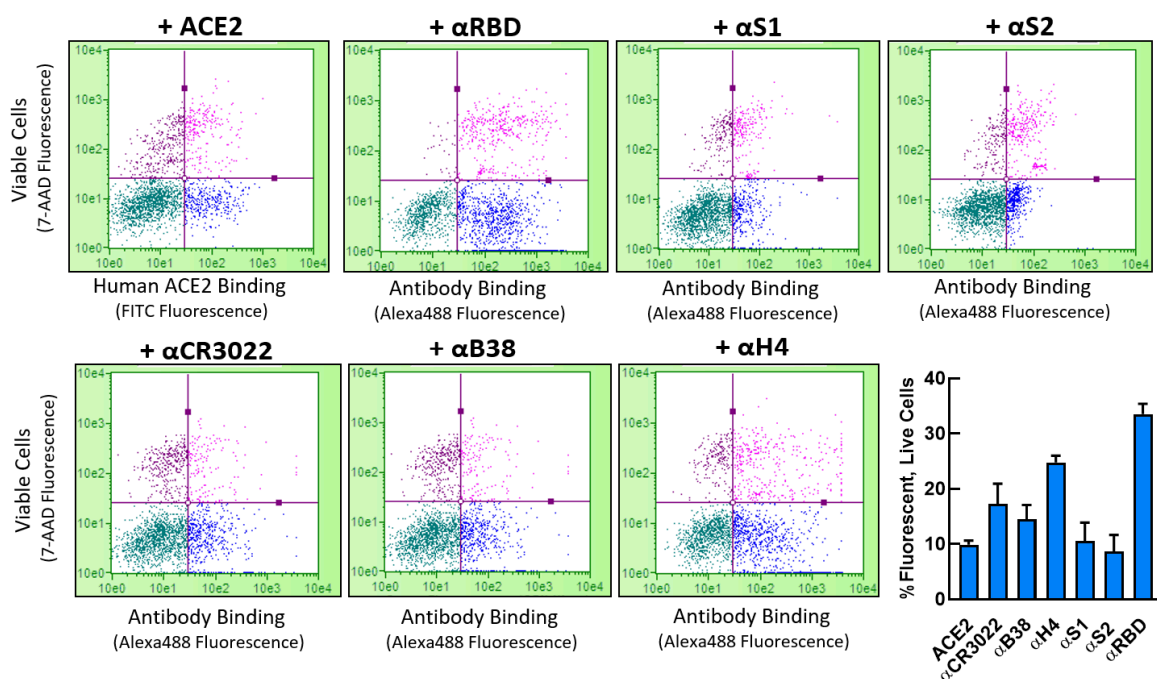
Data Collection		
Electron microscopy equipment	Titan Krios (Thermo Fisher Scientific)	
Voltage (keV)	300	
Detector	K2 Summit	
Energy filter	Gatan GIF, 20 ev slit	
Nominal magnification	165,000 x	
Pixel size (Å)	0.435 (super-resolution)	
	Grid 1	Grid 2
Electron dose (e <sup>-</sup> /Å <sup>2</sup> )	50.32	50.12
Dose rate (e <sup>-</sup> /Å <sup>2</sup> /sec)	8.4	8.33
Defocus range (μm)	-1.2 to -3.4	-1.2 to -3.4
Number of collected micrographs	10,422	17,279
Number of selected micrographs	27,701	
3D Reconstruction		
Software	Warp, Relion	
Number of used particles	58,295	
Symmetry imposed	C3	
Global resolution (Å)		
Fourier shell correction = 0.143	3.29	
Applied B factor (Å <sup>2</sup> )	-50	
Refinement		
Software	Phenix, Coot	
Protein residues	2,919	
Map correlation coefficient	0.82	
Root mean square deviation		
Bond length (Å)	0.011	
Bond angles (°)	0.962	
Ramachandran plot statistics (%):		
Preferred	90.4	
Allowed	9.59	
Outlier	0	
Poor rotamers (%)	11.06	
MolProbity score	2.96	
EMRinger score	2.23	
Clashscore (all atoms)	13.23	



## 4. RESULTS AND DISCUSSION

To confirm surface expression of untagged P2 S as well as the ability of P2 S to bind to human ACE2, flow cytometry experiments were performed on nonpermeabilized cells (Figure 1). Antibodies to the RBD, S1, and S2 were pre-incubated with Alexa-488 anti-IgG Fab for staining, and a nucleic acid dye was used to separate live and dead cells. To confirm binding of human ACE2, P2 S-expressing cells were labeled with the extracellular domain of human ACE2 pre-incubated with a FITC-labeled antibody against an affinity tag on the ACE2. Finally, anti-RBD human neutralizing antibodies B38 and H4 isolated from a COVID-19 convalescent patient (Wu et al, 2020) and the anti-RBD therapeutic antibody CR3022 (Yuan et al, 2020) were similarly confirmed to bind the surface-expressed P2 S.

**Figure 1. Binding to Cell Surface-Expressed Recombinant P2 S**

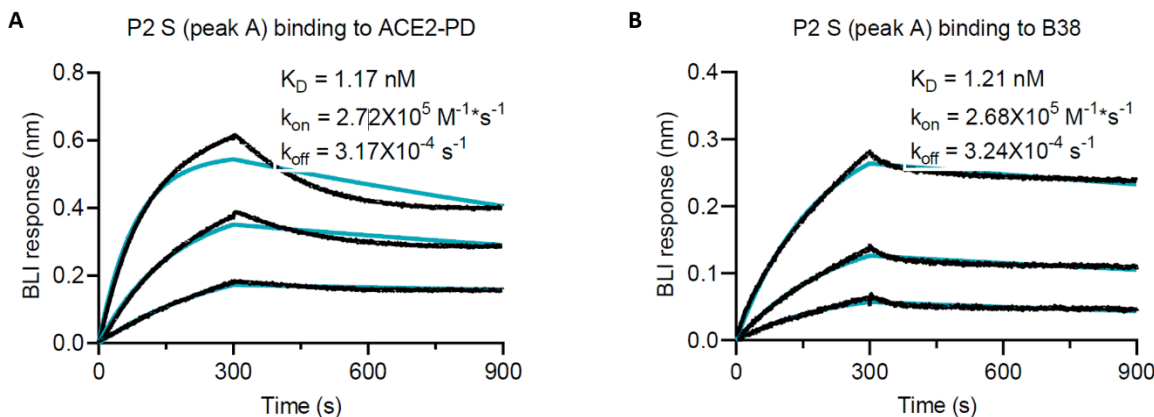


P2 S antigen was expressed in Expi293F cells, and surface expression confirmed by staining with antibodies against the RBD, S1, and S2 regions of the full-length S protein. Human ACE2 peptidase domain as well as the therapeutic antibody CR3022 and two neutralizing antibodies isolated from a COVID-19 convalescent patient, B38 and H4, were further confirmed to bind to surface express P2 S. The nucleic acid dye 7-AAD was used identify viable cells (lower quadrants in flow plots). Binding to surface expressed P2 S over background in live cells is quantified across replicates in the bar graph.

For structural and biophysical characterization, P2 S was expressed in Expi293F cells from DNA that encodes the same amino acid sequence as BNT162b2 RNA, with the addition of a C-terminal TwinStrep tag for affinity purification. Following purification, as described in Methods, P2 S eluted as three distinct peaks in 0.02% NP-40 as previously reported (Cai et al, 2020). Protein from the first peak of a size exclusion column, containing intact P2 S and dissociated S1 and S2, was assayed by biolayer interferometry (Figure 2). The trimeric

P2 S bound to the human ACE2-PD, and an anti-RBD human neutralizing antibody B38 with high affinity (apparent  $K_D = 1$  nM).

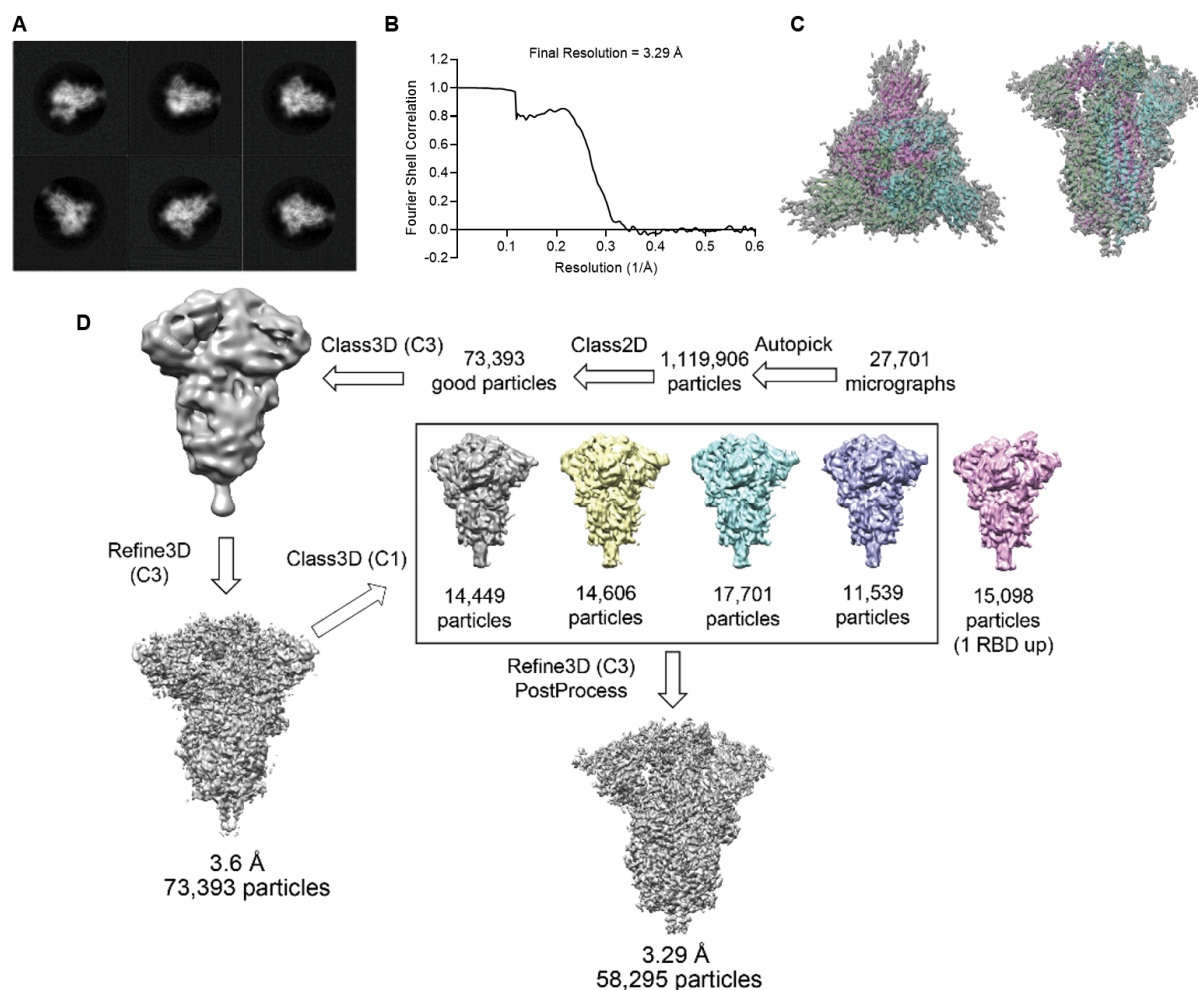
**Figure 2. Biolayer Interferometry Sensorgrams for Binding of P2 S to ACE2-PD and B38 mAb**



P2 S with a C-terminal TwinStrep tag expressed in Expi293F cells, was detergent solubilized and purified by affinity and size exclusion chromatography. Protein from the first peak of a size exclusion column, containing intact P2 S and dissociated S1 and S2, was assayed by biolayer interferometry on an Octet RED384 (FortéBio) at 25 °C in running buffer consisting of 25 mM Tris pH 7.5, 150 mM NaCl, 1mM EDTA and 0.02 % NP-40. Sensorgrams showing the binding kinetics of TwinStrep-tagged P2 S to immobilized **A**, human ACE2-PD and **B**, B38 monoclonal antibody. The highest concentration tested for P2 S was 71 nM with 2 more 3-fold dilutions. The binding curves were globally fit to a 1:1 Langmuir binding model with  $R^2$  values greater than 0.95. Actual binding data (black) and the best fit of the data to a 1:1 binding model (green). Apparent kinetic parameters are provided in the graphs.

Purified TwinStrep-tagged P2 S was characterized structurally using cryoEM. 2D classification of particles from cryoEM data revealed a particle population that closely resembles the prefusion conformation of SARS-CoV-2 spike protein (Figure 3A). Processing and refinement of this dataset yielded a high-quality 3D map with a nominal resolution of 3.29 Å (Figure 3B), into which a previously published atomic model (PDB ID: 6VSB) was fitted and rebuilt. The rebuilt model (Figure 3C) shows good agreement with reported structures of prefusion full-length wild type S (Cai et al, 2020) and its ectodomain with P2 mutations (Wrapp et al, 2020). Three-dimensional classification of the dataset (Figure 3D) showed a class of particles that was in the one RBD ‘up’ (accessible for receptor binding), two RBD ‘down’ (closed) conformation and represented 20.4% of the trimeric molecules. The remainder were in the all RBD ‘down’ conformation. The RBD in the ‘up’ conformation was less well resolved than other parts of the structure, suggesting conformational flexibility and a dynamic equilibrium between RBD ‘up’ and RBD ‘down’ states as also suggested by others (Cai et al, 2020; Henderson et al, 2020).

**Figure 3. CryoEM P2 S Structure at 3.29 Å Resolution**



**A.** Representative 2D class averages of TwinStrep-tagged P2 S particles extracted from cryoEM micrographs. Box edge: 39.2 nm. **B.** Fourier shell correlation curve from RELION gold-standard refinement of the P2 S trimer. **C.** 3.29 Å cryoEM map of TwinStrep-tagged P2 S, with fitted atomic model, showing top (perpendicular to the three-fold axis) and side (parallel to the three-fold axis) views. CryoEM model is based on PDB 6VSB and was fitted into the structure using manual rebuilding in Coot and real-space refinement in Phenix. ~28,000 micrographs were collected using a Titan Krios electron microscope operating at 300 kV accelerating voltage, and image processing and 3D reconstructions were performed using Warp and RELION. **D.** Flowchart for cryo-EM data processing of the complex, showing 3D class averages. Maps of P2 S produced by 3D classification indicate some heterogeneity in positioning of the RBD domains. Percentages of the particle population represented in each class are indicated below the models.

## 5. CONCLUSION

We demonstrate that the BNT162b2 RNA sequence encodes a recombinant P2 S that can authentically present the ACE2 binding site and other epitopes targeted by SARS-CoV-2 neutralizing antibodies.

Binding of cell surface expressed P2 S to human ACE2 receptor and a panel of human neutralizing mAbs was confirmed in cells using flow cytometry. Protein expressed from DNA with the BNT162b2-encoded P2 S amino acid sequence was confirmed to be in the prefusion conformation by cryo-EM. This analysis showed that the antigenically important RBD can assume the 'up' conformation, with the receptor binding site, rich in neutralizing epitopes, accessible in a proportion of the molecules (Zost et al, 2020). The alternative states observed reflect a dynamic equilibrium between RBD 'up' and 'down' positions (Cai et al, 2020; Henderson et al, 2020). Binding of expressed and purified P2 S to ACE2 and a neutralizing monoclonal antibody further demonstrates its conformational and antigenic integrity.

## 6. DEVIATIONS

N/A

## 7. REFERENCES

Adams PD, Afonine PV, Bunkoczi G, et al. PHENIX: a comprehensive Python-based system for macromolecular structure solution. *Acta Crystallogr D Biol Crystallogr*. 2010; 66:213-21.

Brouwer PJM, Caniels TG, van der Straten KJ, et al. Potent neutralizing antibodies from COVID-19 patients define multiple targets of vulnerability. *Science* 2020;369(6504):643-50.

Cai Y, Zhang J, Xiao T, et al. Distinct conformational states of SARS-CoV-2 spike protein. *Science* 2020; 369:1586-92.

Emsley P, Lohkamp B, Scott WG, et al. Features and development of Coot. *Acta Crystallogr D Biol Crystallogr*. 2010;66(Pt 4)(Apr):486-501.

Henderson R, Edwards RJ, Mansouri K, et al. Controlling the SARS-CoV-2 spike glycoprotein conformation. *Nat Struct Mol Biol* 2020; 27:925-33.

Liu L, Wang P, Nair MS, et al. Potent neutralizing antibodies against multiple epitopes on SARS-CoV-2 spike. *Nature* 2020;584(7821):450-6.

Pallesen J, Wang N, Corbett KS, et al. Immunogenicity and structures of a rationally designed prefusion MERS-CoV spike antigen. *Proc Natl Acad Sci USA* 2017;114(35)(08):E7348-E7357.

Robbiani DF, Gaebler C, Muecksch F, et al. Convergent antibody responses to SARS-CoV-2 in convalescent individuals. *Nature* 2020, 584, 437-42.

Tegunov D, Cramer P. Real-time cryo-electron microscopy data preprocessing with Warp. *Nat Methods* 2019; 16:1146–52.

Wrapp D, Wang N, Corbett KS, et al. Cryo-EM structure of the 2019-nCoV spike in the prefusion conformation. *Science* 2020;367(6483)(03):1260-3.

Wu Y, Wang F, Shen C, et al. A noncompeting pair of human neutralizing antibodies block COVID-19 virus binding to its receptor ACE2. *Science* 2020;368(6496)(06):1274-8.

Yuan M, Wu NC, Zhu X, et al. A highly conserved cryptic epitope in the receptor binding domains of SARS-CoV-2 and SARS-CoV. *Science* 2020;368(6491)(05):630-3.

Zhou M, Zhang X, Qu J. Coronavirus disease 2019 (COVID-19): a clinical update. *Front Med* 2020; 14:126-135.

Zivanov J, Nakane T, Forsberg BO, et al. New tools for automated high-resolution cryo-EM structure determination in RELION-3. *eLife* 2018;7:e42166.

Zost SJ, Gilchuk P, Chen RE, et al. Rapid isolation and profiling of a diverse panel of human monoclonal antibodies targeting the SARS-CoV-2 spike protein. *Nat Med* 2020;26:1422-7.4.

## Document Approval Record

**Document Name:**

VR-VTR-10741

**Document Title:**

Structural and Biophysical Characterization of SARS-CoV-2 Spike Glycoprotein (P2 S) as a Vaccine Antigen

**Signed By:**

**Date(GMT)**

**Signing Capacity**

(b) (6)

26-Dec-2020 20:46:27

Final Approval

26-Dec-2020 21:51:07

Author Approval

27-Dec-2020 01:00:37

Scientific Review

27-Dec-2020 02:23:18

Quality Assurance Approval

090177e195e446ea\Approved\Approved On: 27-Dec-2020 02:23 (GMT)